



Preparation of chitosan/cellulose acetate composite nanofiltration membrane for wastewater treatment

Azadeh Ghaee^{a,*}, Mojtaba Shariaty-Niassar^b, Jalal Barzin^c, Takeshi Matsuura^d, Ahmad Fauzi Ismail^e

^aFaculty of New Sciences and Technologies, Department of Life Science Engineering, University of Tehran, P.O. Box 14395-1561, Tehran, Iran, email: ghaee@ut.ac.ir

^bSchool of Chemical Engineering, College of Engineering, University of Tehran, P.O. Box 11365-4563, Tehran, Iran, email: mshariat@ut.ac.ir

^cDepartment of Biomaterials, Iran Polymer and Petrochemical Institute, P.O. Box 14965/115, Tehran, Iran, email: j.barzin@ippi.ac.ir

^dIndustrial Membrane Research Laboratory, Department of Chemical and Biological Engineering, University of Ottawa, Ottawa, Ont. K1N 6N5, Canada, email: matsuura@eng.uottawa.ca

^eAdvanced Membrane Technology Research Centre (AMTEC), Universiti Teknologi Malaysia, Skudai, Johor 81310, Malaysia, email: afauzi@utm.my

Received 21 February 2015; Accepted 21 June 2015

ABSTRACT

A chitosan/cellulose acetate (CA) composite membrane is prepared in this study. The effect of varying CA concentration on membrane morphology and performance is studied by using scanning electron microscopy and the composite membrane is characterized by differential scanning calorimetry and thermal gravimetric analysis. Molecular weight cut-off of the composite membrane is found to be 830 Da, which is in the range of nanofiltration. The rejection for copper from a common effluent treatment plant wastewater is observed to be 81.03% at 506.5 kPa applied pressure. The mean pore size is calculated to be 0.78 nm.

Keywords: Nanofiltration; Chitosan; Cellulose acetate; Thermal analysis; Composite membrane

1. Introduction

Due to potentially unacceptable ecological risks to plants, animals, and micro-organism, as well as carcinogenic risks to humans, heavy metal contamination of water resources has attracted attention for the past many years [1]. Metal ions can be removed from aqueous effluents by conventional techniques, such as reverse osmosis (RO) and chemical precipitation, [2–4] but these methods are costly and incapable of removing trace levels of heavy metal ions from wastewater

[4]. Membrane separation is a promising technology with lower energy cost for the selective separation of heavy metal ions [5].

Nanofiltration (NF), a pressure-driven membrane process, has practical applications in water treatment [6–8]. The mechanism is based on sieving and the Donnan effect [9–12]. It can be operated at relatively low pressures (0.3–1.5 MPa) and has high rejection of multivalent ions [9]. The molecular weight cut-off (MWCO) of NF ranges from 200 to 2,000 Da, a set of values intermediate to those of ultrafiltration (UF) and RO [9–13].

*Corresponding author.

Cellulose acetate (CA) was one of the first membrane polymers to be used for aqueous-based separation, and used as both RO and UF membrane material. This material is still commonly used, because it has a natural origin with hydrophilic property and maintains high mechanical strength during membranes fabrication and process. However, a major drawback is lack of reactive functional groups on the CA polymer backbones to enhance the separation efficiency of the membranes and this polymer is not suitable for adsorptive separation that works on the principle of affinity [14–16].

To obtain higher selectivity and higher flux, CA membrane modifications are often required [16,17]. One such modification involves blending CA with chitosan (CS) [17–20]. Boricha and Murthy [17] prepared N,O-carboxy methyl CS (CMC)/CA blend NF membrane for chromium and copper ions separation, and their rejections were 83.4 and 73.6%, respectively. The addition of CS increases membrane hydrophilicity by introducing reactive sites (amino and hydroxyl groups) in the membrane material. Further, CS composite membranes are easily regenerated, and have higher flux and retention and antifouling properties [21,22]. Musale and Kumar [21] prepared CS/polyacrylonitrile composite UF membrane. Also, Miao et al. [23] fabricated N,O-carboxy methyl CS/polyether sulfone composite membrane. Daraei et al. [24] fabricated thin film composite membrane by mixed matrix nanoclay/CS on PVDF microfiltration support for dye removal. However, polymers like polysulfone, polyacrylonitrile, and polyvinylidene fluoride are hydrophobic materials and the structural stability of CS composite membranes with these sublayers is not acceptable to endure the long experimental condition and significant difference in surface tension caused segregation of these layers under swelling condition. [25]. So, in this study, CS/CA composite membranes are prepared for metal ion removal, that is rarely reported in the literature. The pure water permeability, MWCO, rejection behavior, characteristics of CS/CA composite NF membranes, and the effects of CA concentration on membrane morphology and performance are studied.

2. Experimental

2.1. Materials

CA was supplied by Aldrich Co. N-methyl pyrrolidone (NMP) (Merck) was used as the solvent. CS was purchased from Chitotech. All other chemicals (glutaraldehyde, acetic acid, sodium hydroxide, cupric

sulfate, and polyethylene glycol (PEG)) were of analytical grade and used without further purification.

2.2. Membrane preparation

The substrate CA membranes were prepared by dissolving various amounts of CA (i.e. 15, 18, and 20% w/w) in NMP solvent containing PEG (600 Da) (10% w/w of solution). After aeration, the CA solution was poured onto a flat surface. A proper membrane thickness was formed using a 200- μm slot applicator. After pouring the solution (without solvent evaporation), the process of coagulation was carried out in distilled water.

To prepare the CS/CA composite membrane, CS solution (0.5% (w/w)) in aqueous acetic acid (10% (w/w)) was filtered. The CA membrane prepared from the dope of 15% w/w CA was immersed in eight consecutive solutions with different concentrations of ethanol and n-hexane, i.e. 25, 50, 75, and 100% of ethanol in water and then 25, 50, 75, and 100% of n-hexane in ethanol for solvent exchange before the membrane was dried. The substrate membrane was then immersed in the CS solution for 3 min, and dried at 25°C. Cross-linking was carried out by immersing the dry membrane into a 0.25% (w/w) glutaraldehyde aqueous solution, at 25°C for 30 min, followed by washing with distilled water to remove the unreacted glutaraldehyde residues. Finally, the membranes were dried by a filter paper.

2.3. Membrane performance

Pure water permeation for CA sublayers was measured using a flow through cell (effective membrane area, $20 \times 10^{-4} \text{ m}^2$) at 25°C at different operating pressures (i.e. 202.6, 303.9, and 506.5 atm).

The permeation performance was studied for composite membrane by determining the fluxes, and rejections for CuSO_4 solution with a concentration of either 50, or 100 mg L^{-1} , and at an operating pressure of 506.5 kPa. Flux (F) and rejection (R) were determined as follows.

F was calculated by Eq. (1):

$$F = \frac{V}{A \times t} \quad (1)$$

where F ($\text{Lm}^{-2} \text{ h}^{-1}$) is the flux, A (m^2) is the effective area of the membrane; t (h) and V (L) are the time and the volume of permeate through the membrane, respectively. R was calculated by Eq. (2):

$$R (\%) = \left(1 - \frac{C_P}{C_F}\right) \times 100 \quad (2)$$

where C_P (mg L^{-1}) and C_F (mg L^{-1}) are the copper concentrations in permeate and feed streams, respectively. All reported data are the mean values of three replicates.

2.4. Molecular weight cut-off (MWCO)

MWCO of the composite membrane was determined using the rejection data for PEG of various molecular weights (200–1,500 Da). The feed PEG concentration was $1,000 \text{ mg L}^{-1}$. The concentrations of PEG in the feed and permeate were measured by total organic carbon analyzer (Model DC-190).

2.5. Characterization

2.5.1. Attenuated total reflectance–Fourier-transform infrared (ATR-FTIR) Analysis

ATR-FTIR analysis (Bruker, Equinox 55) was used to characterize the surface chemistry of membranes made of CA and CS/CA membranes.

2.5.2. Scanning electron microscopy (SEM)

Membranes were fractured in liquid nitrogen for SEM observation, before their cross sections were covered with a thin layer of gold using a sputter coater (SCDOOS–Baltec, Switzerland). The cross sections were observed by a SEM (XL30-Philips-Netherlands).

2.5.3. Contact angle

Hydrophobicity of CA and CS/CA membranes were measured by water contact angle analyzer (Contact Angle Measurement System G10, LBI02, and KRUSS).

2.5.4. Thermal analysis

Thermal gravimetric analysis (TGA) measures the weight of a polymer, as a function of temperature, or time, while the sample is subjected to a controlled temperature program in a controlled atmosphere [26]. CS/CA composite membrane was analyzed using the TGA analyzer (Polymer laboratories, United Kingdom) under a nitrogen atmosphere. The heating rate was $10^\circ\text{C}/\text{min}$, from 30 to 600°C .

Differential scanning calorimetry (DSC), the most popular thermal analysis technique, measures

difference in rate of heat transferred to a sample, and a reference as a function of temperature, while the sample is subjected to a controlled temperature program [26]. The composite membrane was analyzed by DSC, using a Netzsch DSC 200/F3 Maia at a rate of $10^\circ\text{C min}^{-1}$, ranging from 25 to 350°C under a nitrogen atmosphere.

2.5.5. Atomic absorption experiments

The concentrations of metal ions were measured by a flame atomic absorption spectrophotometer (Varian AA Model 240). All the reported copper concentrations are the mean values of three replicates.

3. Results and discussion

3.1. ATR-FTIR analysis

ATR spectrum of CA and CS/CA was shown in Fig. 1. A band at 940 cm^{-1} corresponds to β -linked glucan structure. The absorption bands at $1,052$ and $1,190 \text{ cm}^{-1}$ are attributed to C–O bending and C–O asymmetric stretching. An absorption bands at $1,235$, $1,350$, and $1,752 \text{ cm}^{-1}$ correspond to C–C–O stretching of acetate, C–H bending, and C=O stretching, respectively. The absorption bands at $2,933$ and $3,512 \text{ cm}^{-1}$ belong to CH₂, CH₃ asymmetric stretching, and OH stretching of CA hydroxyl groups. Another peak at $1,670 \text{ cm}^{-1}$ is attributed to O–H stretching and bending vibrations of molecular water [27,28]. ATR spectrum of CS/CA is similar to CA, except an absorption band at $1,572 \text{ cm}^{-1}$ belongs to N–H bending in amide II of CS [29].

3.2. SEM analysis

Fig. 2(a)–(c) show the SEM images of substrate CA membranes with various CA concentrations. When CA concentration was increased, the solution viscosity increased, resulting in slower phase inversion and therefore smaller membrane pore sizes. All the membrane sublayers had asymmetric structures, while the membrane with 15 wt.% CA (Fig. 2(a)) showed a channel-like structure, those with higher CA concentrations (18 and 20 wt.%, Fig. 2(b) and (c)) exhibited finger-like and tear-like structures with smaller voids and a larger portion of sponge-like texture. Similar results were observed by Stropnik et al., Barth et al. and Barzin et al. for polyamide, polysulfone and poly (ether sulfone) flat-sheet membranes [30–32].



Fig. 1. ATR spectrum of CA and CS/CA membranes.

3.3. Membrane performance

3.3.1. Substrate membrane

The membrane performance data at different CA concentrations are reported in Table 1. When CA concentration is increased, water flux and water permeability are decreased. These results might be expected based on the SEM images, as the 15 wt.% CA membrane has channel-like structures with larger and more frequent pores, while the 20 wt.% CA membrane has fewer and smaller finger-like voids and a more evenly distributed sponge-like structure (compare Fig. 2(b) and (c)). Table 1 also shows that the flux increases for higher operating pressure.

3.3.2. CS/CA composite membrane

The substrate membrane with 15% CA was chosen as the support layer of the composite membrane. Although this membrane is very porous it has a sponge-like layer at the top and has sufficiently high mechanical stability to support the composite membrane. Further, its large pores allow the highest water flux among the substrate membranes.

The membrane performance is reported in Table 2. The substrate layer retention is about 18.5%, while for the composite membrane with 100 ppm initial CS concentration, it is 81.03%. The contact angles of CA and CS/CA are 61° and 48°, respectively. The water flux in the composite layer was much lower than that of the substrate layer due to the upper CS dense layer. Boricha and Murthy [17] prepared an N,O carboxymethyl CS

(NOCC)/CA blend NF membrane for wastewater treatment. They reported that composite membrane copper ion rejection and water flux were 72.6% and 70 Lm⁻² h⁻¹, respectively. Musale and Kumar [21] prepared CS/ polyacrylonitrile composite NF membrane with 6.3 Lm⁻² h⁻¹ flux and 87.7% rejection. Huang et al. [33] fabricated quaternized CS/ polyacrylonitrile composite NF membrane with 6.8 Lm⁻² h⁻¹ flux and 43.7% rejection. N,O carboxymethyl CS (NOCC)/ polysulfone NF membrane which was prepared by Miao et al. [34], has 4.7 Lm⁻² h⁻¹ flux and 28.2% rejection. Balanya et al. [35] tested flat NF membranes made by Koch (SelRO[®] MPF-36) and a ceramic membrane made by Tami (CERAM INSIDE[®]) for copper ion rejection. They found out that copper ion rejections were 40 and 84% for MPF-36 at an operating pressure of 9 bar and CERAM membrane at an operating pressure of 14 bar, respectively.

3.4. Thermal analysis

Fig. 3 shows DSC thermogram curves for CS, CA, and CS/CA composite membranes. All three curves share a broad endothermic event between ambient temperature and 100°C. This event is attributed to water desorption from the membrane structures. The thermogram for the CS membrane has a sharp exothermic peak at 268°C due to CS decomposition. The endothermic peak at 100°C indicates the presence of water in the film [36,37].

The DSC thermogram for the CA membrane has an exothermic peak at 202°C due to CA crystallization,

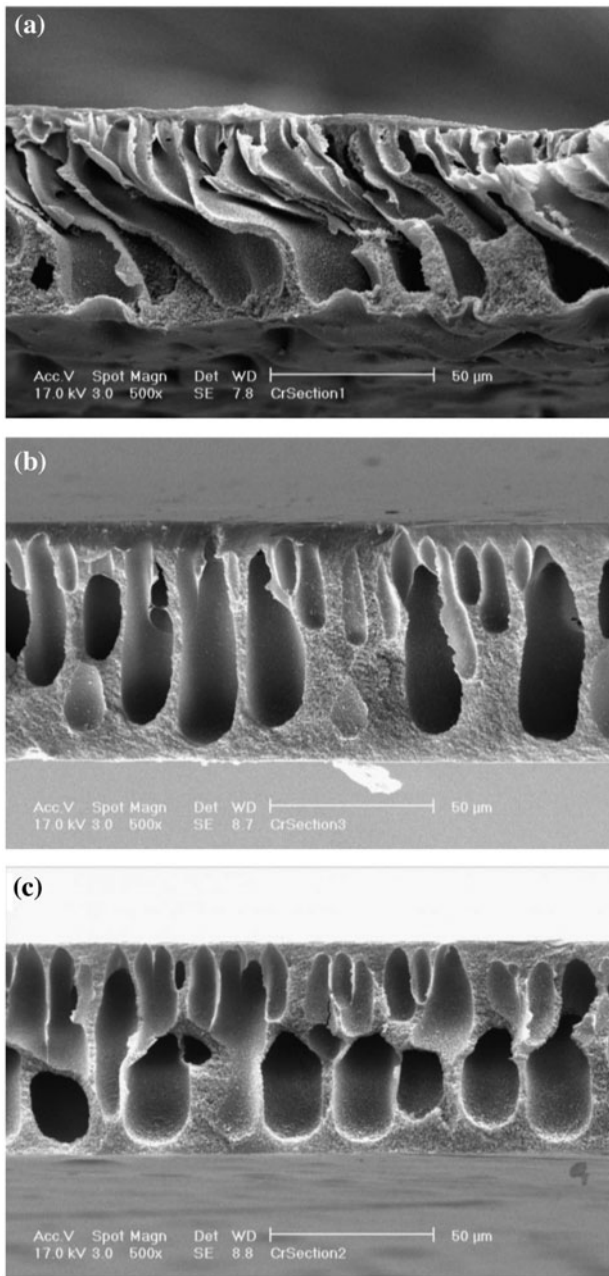


Fig. 2. CA sublayer with (a) 15%, (b) 18%, and (c) 20% CA.

Table 1
Substrate membrane water flux

CA concentration (wt.%)	Water flux (Lm ² h ⁻¹)		
	2 atm	3 atm	5 atm
15	309.2	422.6	591.3
18	186.3	254.9	375.7
20	91.5	145.1	237.8

Table 2
Composite and substrate membrane performance

		Initial copper concentration (mg L ⁻¹)	
		50	100
Substrate layer	Flux (Lm ² h ⁻¹)	–	591.3
	Retention (%)	–	18.50
Composite membrane	Flux (Lm ² h ⁻¹)	4.37	4.37
	Retention (%)	80.49	81.03

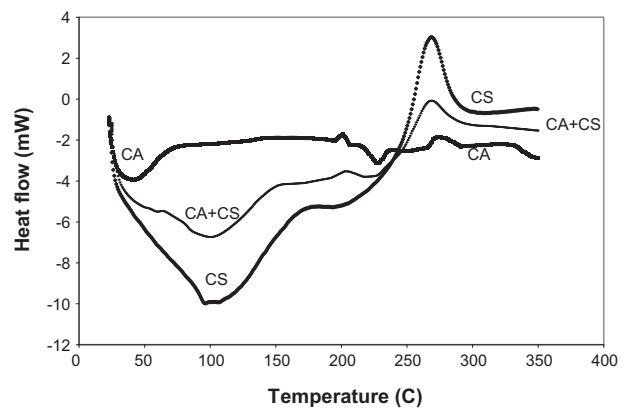


Fig. 3. DSC curves of CA, CS, and CA/CS membranes.

and an endothermic peak at 229°C due to the melting of sample. The exothermic peak at around 274°C can be attributed to the thermal decomposition of the membrane [38,39].

The DSC thermogram for the CS/CA composite membrane shows that a peak at 205°C due to CA crystallization, and one at 269°C due to CS degradation. Thus, the DSC analysis confirms the existence of a CS layer on the CA sublayer.

The TGA curve for the CS membrane (Fig. 4) shows that the first weight loss of 11.7%, due to water vaporization, occurred above 100°C. The second loss corresponding to CS decomposition began at 181.8°C [40]. Ash percent in the CS membrane was about 29.8%. The TGA curve for the CA membrane shows about 2% water loss and CA decomposition starting at 264°C [38,39]. Finally, in this TGA curve is the carbonization of the degraded products to ash (12.45%). In the CS/CA composite membrane, water loss was about 8%, and membrane degradation started at 207.5°C due to the presence of CS. Final ash percent is about 20%. Like the DSC analysis, these TGA curves

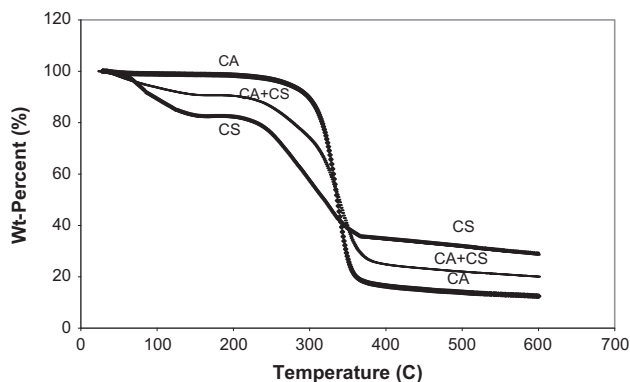


Fig. 4. Thermogravimetric analysis of CA, CS, and CA/CS membranes.

confirm the presence of a CS layer in the composite membrane.

3.5. MWCO of the CS/CA composite NF membrane

To determine MWCO, a set of reference solutes in the molecular weight range of 200–1,500 Da (PEGs 200, 400, 600, 1,000, and 1,500 Da) was chosen and separation experiments were conducted at a concentration of $1,000 \text{ mg L}^{-1}$. MWCO is defined as the molecular weight of organic solutes with retention of 90%. Fig. 5 plots the rejection of solutes vs. their molecular weight for the CS/CA membrane. The MWCO of this membrane was determined by interpolation to be approximately 830.74 Da, which is in the NF range.

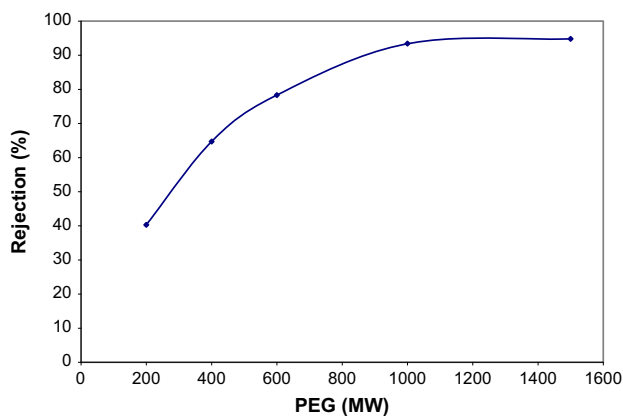


Fig. 5. Rejection vs PEG molecular weight for composite membrane.

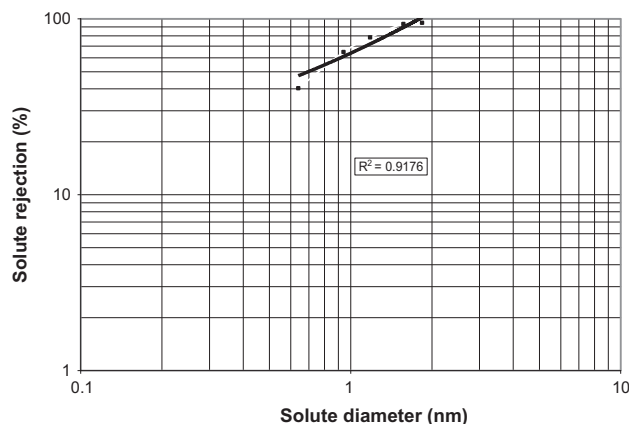


Fig. 6. Rejection vs. PEG solute diameter plotted on log-normal basis for composite membrane.

3.6. Mean pore size and pore size distribution

Solute diameter was obtained by Eq. (3) from the molecular weight of PEG.

$$a = 16.73 \times 10^{-10} \times M^{0.557} \quad (3)$$

where a (cm) is solute diameter and M is the molecular weight of PEG (Da). When solute separation is plotted vs. solute diameter on a log-normal probability paper, a straight line is yielded as reported [41]. From this log-normal plot (Fig. 6), mean solute size can be calculated as solute diameter corresponding to retention of 50%. The mean pore size of the composite membrane is 0.78 nm, which is in the range of NF membranes.

4. Conclusions

CS and CA are hydrophilic materials that can be used to create a structurally stable composite membrane that withstand lengthily experimental conditions. By increasing CA concentration, finger-like structures appeared instead of channel-like configurations. It is due to a slow exchange rate between solvent and non-solvent, resulting in an increase in the viscosity of the polymer solution. A CA membrane with 15% polymer concentration had the highest water permeability and selected as the substrate for a composite membrane. DSC and TGA analysis confirmed the composite membrane formation. The CS/CA composite membrane had 81.03% retention for copper ions. The MWCO of the resultant membrane was 830.74 Da (in the NF range), and the mean pore size was 0.78 nm.

Nomenclature

F	—	flux ($\text{Lm}^{-2} \text{h}^{-1}$)
A	—	area (m^2)
t	—	time (h)
V	—	volume (L)
R	—	rejection
C_P	—	concentrations of the permeation (mg L^{-1})
C_F	—	concentrations of the feed (mg L^{-1})
a	—	solute diameter (cm)
M	—	molecular weight

Subscripts

P	—	permeation
F	—	feed

References

- [1] A.T. Paulino, F.A.S. Minasse, M.R. Guilherme, A.V. Reis, E.C. Muniz, J. Nozaki, Novel adsorbent based on silkworm chrysalides for removal of heavy metals from wastewaters, *J. Colloid Interface Sci.* 301 (2006) 479–487.
- [2] S.H. Lin, R.S. Juang, Heavy metal removal from water by sorption using surfactant-modified montmorillonite, *J. Hazard. Mater.* 92 (2002) 315–326.
- [3] S.J. Kim, K.H. Lim, Y.G. Park, J.H. Kim, S.Y. Cho, Simultaneous removal and recovery of cadmium and cyanide ions in synthetic wastewater by ion exchange, *Korean J. Chem. Eng.* 18 (2001) 686–691.
- [4] J.B. Brower, R.L. Ryan, M. Pazirandeh, Comparison of ion-exchange resins and biosorbents for the removal of heavy metals from plating factory wastewater, *Environ. Sci. Technol.* 31 (1997) 2910–2914.
- [5] H. Okushita, T. Shimidzu, Membrane separation of Ga^{3+} by selective interaction of Ga^{3+} with N-octadecanoyl-N-phenylhydroxylamine, *J. Membr. Sci.* 116 (1996) 61–65.
- [6] W.R. Bowen, J.S. Welfoot, Modelling of membrane nanofiltration-pore size distribution effects, *Chem. Eng. Sci.* 57 (2002) 1393–1407.
- [7] B.A.M. Al-Rashdi, D.J. Johnson, N. Hilal, Removal of heavy metal ions by nanofiltration, *Desalination* 315 (2013) 2–17.
- [8] J.A. Otero, O. Mazarrasa, A. Otero Fernandez, A. Fernandez, A. Hernandez, A. Marato-Valiente, Treatment of wastewater. Removal of heavy metals by nanofiltration, Case study: Use of TFC membranes to separate Cr(VI) in industrial pilot plant, *Procedia Eng.* 44 (2012) 2020–2022.
- [9] X.L. Wang, C. Zhang, P. Ouyang, The possibility of separating saccharides from a NaCl solution by using nanofiltration in diafiltration mode, *J. Membr. Sci.* 204 (2002) 271–281.
- [10] S. Szoke, G. Patzay, L. Weiser, Characteristics of thin-film nanofiltration membranes at various pH-values, *Desalination* 151 (2003) 123–129.
- [11] J.J. Qin, M.H. Oo, H. Lee, B. Coniglio, Effect of feed pH on permeate pH and ion rejection under acidic conditions in NF process, *J. Membr. Sci.* 232 (2004) 153–159.
- [12] C. Martin-Orue, S. Bouhallab, A. Garem, Nanofiltration of amino acid and peptide solutions: Mechanisms of separation, *J. Membr. Sci.* 142 (1998) 225–233.
- [13] S. Hong, M. Elimelech, Chemical and physical aspects of natural organic matter (NOM) fouling of nanofiltration membranes, *J. Membr. Sci.* 132 (1997) 159–181.
- [14] S.H. Choi, Y.C. Nho, G.T. Kim, Adsorption of Pb^{2+} and Pd^{2+} on polyethylene membrane with amino group modified by radiation-induced graft copolymerization, *J. Appl. Polym. Sci.* 71 (1999) 643–650.
- [15] E. Klein, Affinity membranes: A 10-year review, *J. Membr. Sci.* 179 (2000) 1–27.
- [16] O. Kutowy, S. Sourirajan, Cellulose acetate ultrafiltration membranes, *J. Appl. Polym. Sci.* 19 (1975) 1449–1460.
- [17] A.G. Boricha, Z.V.P. Murthy, Preparation of N,O-carboxymethyl chitosan/cellulose acetate blend nanofiltration membrane and testing its performance in treating industrial wastewater, *Chem. Eng. J.* 157 (2010) 393–400.
- [18] C. Liu, R. Bai, Preparation of chitosan/cellulose acetate blend hollow fibers for adsorptive performance, *J. Membr. Sci.* 267 (2005) 68–77.
- [19] C. Liu, R. Bai, Preparing highly porous chitosan/cellulose acetate blend hollow fibers as adsorptive membranes: Effect of polymer concentrations and coagulant compositions, *J. Membr. Sci.* 279 (2006) 336–346.
- [20] C. Liu, R. Bai, Adsorptive removal of copper ions with highly porous chitosan/cellulose acetate blend hollow fiber membranes, *J. Membr. Sci.* 284 (2006) 313–322.
- [21] D.A. Musale, A. Kumar, Effects of surface crosslinking on sieving characteristics of chitosan:poly(acrylonitrile) composite nanofiltration membranes, *Sep. sci. Technol.* 20 (2000) 27–38.
- [22] D.A. Musale, A. Kumar, Formation and characterization of poly(acrylonitrile)/chitosan composite ultrafiltration membranes, *J. Membr. Sci.* 154 (1999) 163–173.
- [23] J. Miao, G. Chen, C. Gao, A novel kind of amphoteric composite nanofiltration membrane prepared from sulfated chitosan (SCS), *Desalination* 181 (2005) 173–183.
- [24] P. Daraei, S.S. Madaeni, E. Salehi, N. Ghaemi, H. Sadeghi Ghari, M.A. Khadivi, E. Rostami, Novel thin film composite membrane fabricated by mixed matrix nanoclay/chitosan on PVDF microfiltration support: Preparation, characterization and performance in dye removal, *J. Membr. Sci.* 436 (2013) 97–108.
- [25] R.Y.M. Huang, R. Pal, G.Y. Moon, Crosslinked chitosan composite membrane for the pervaporation dehydration of alcohol mixtures and enhancement of structural stability of chitosan/polysulfone composite membranes, *J. Membr. Sci.* 160 (1999) 17–30.
- [26] J.D. Menczel, R.B. Prime, *Thermal Analysis of Polymers: Fundamentals and Applications*, John Wiley & Sons, Hoboken, NJ, 2009, pp. 7–314.
- [27] H. Sanaeepur, B. Nasernejad, A. Kargari, Cellulose acetate/nano-porous zeolite mixed matrix membrane for CO_2 separation, *Greenhouse Gas Sci. Technol.* 5 (2015) 291–304.
- [28] A.J.M. Valente, A.Y. Polishchuk, H.D. Burrows, V.M.M. Lobo, Permeation of water as a tool for characterizing the effect of solvent, film thickness and water solubility in cellulose acetate membranes, *Eur. Polym. J.* 41 (2005) 275–281.

- [29] J.Y. Lai, Y.T. Li, T.P. Wang, In vitro response of retinal pigment epithelial cells exposed to chitosan materials prepared with different cross-linkers, *Int. J. Mol. Sci.* 11 (2010) 5256–5272.
- [30] Č. Stropnik, L. Germič, B. Žerjal, Morphology variety and formation mechanisms of polymeric membranes prepared by wet phase inversion, *J. Appl. Polym. Sci.* 61 (1996) 1821–1830.
- [31] C. Barth, M.C. Gonçalves, A.T.N. Pires, J. Roeder, B.A. Wolf, Asymmetric polysulfone and polyethersulfone membranes: Effects of thermodynamic conditions during formation on their performance, *J. Membr. Sci.* 169 (2000) 287–299.
- [32] J. Barzin, C. Feng, K.C. Khulbe, T. Matsuura, S.S. Madaeni, H. Mirzadeh, Characterization of polyethersulfone hemodialysis membrane by ultrafiltration and atomic force microscopy, *J. Membr. Sci.* 237 (2004) 77–85.
- [33] R.Y.M. Huang, G. Chen, M. Sun, Y. Hu, C. Gao, Preparation and characteristics of quaternized chitosan/poly(acrylonitrile) composite nanofiltration membrane from epichlorohydrin cross-linking, *Carbohydr. Polym.* 70 (2007) 318–323.
- [34] J. Miao, G. Chen, C. Gao, C. Lin, D. Wang, M. Sun, Preparation and characterization of N,O-carboxymethyl chitosan (NOCC)/polysulfone (PS) composite nanofiltration membranes, *J. Membr. Sci.* 280 (2006) 478–484.
- [35] T. Balanyà, J. Labanda, J. Llorens, J. Sabaté, Separation of metal ions and chelating agents by nanofiltration, *J. Membr. Sci.* 345 (2009) 31–35.
- [36] S. Tripathi, G.K. Mehrotra, P.K. Dutta, Physicochemical and bioactivity of cross-linked chitosan-PVA film for food packaging applications, *Int. J. Biol. Macromol.* 45 (2009) 372–376.
- [37] C.E. Orrego, J.S. Valencia, Preparation and characterization of chitosan membranes by using a combined freeze gelation and mild crosslinking method, *Bioprocess. Biosyst. Eng.* 32 (2009) 197–206.
- [38] H.S. Barud, A.M. de Araújo Júnior, D.B. Santos, R.M.N. de Assunção, C.S. Meireles, D.A. Cerqueira, G.R. Rodrigues Filho, C.A. Ribeiro, Y. Messaddeq, S.J.L. Ribeiro, Thermal behavior of cellulose acetate produced from homogeneous acetylation of bacterial cellulose, *Thermochim. Acta* 471 (2008) 61–69.
- [39] F.J. Rodriguez, J.M. Galotto, A. Guarda, J.E. Bruna, Modification of cellulose acetate films using nanofillers based on organoclays, *J. Food Eng.* 110 (2012) 262–268.
- [40] H.H. Oo, K. Naing, K.M. Naing, T.T. Aye, N. Wymr, Electrochemical and thermal studies of prepared conducting chitosan biopolymer film, *J. Myan. Acad. Arts Sci.* 3 (2005) 62–72.
- [41] S. Singh, K.C. Khulbe, T. Matsuura, P. Ramamurthy, Membrane characterization by solute transport and atomic force microscopy, *J. Membr. Sci.* 142 (1998) 111–127.